[11] H. K. Khalil, *Nonlinear Systems*, 3rd ed. Englewood Cliffs, NJ: Prentice-Hall, 2002.
[12] O. Kolesnichenko and A. S. Shiriaev, "Partial stabilization of underactuated Euler–Lagrange systems via a class of feedback transformations," *Syst. Control Lett.*, vol. 45, no. 2, pp. 121–132, 2002.
[13] Y. Michitsuji, H. Sato, and M. Yamakita, "Giant swing via forward upward circling of the acrobat-robot," *Proc. Amer. Control Conf.*, pp. 326–3266, 2001.
[14] R. Ortega, M. W. Spong, F. Gomez-Estern, and G. Blankenstein, "Stabilization of a class of underactuated mechanical systems via interconnection and damping assignment," *IEEE Trans. Autom. Control*, vol. 47, no. 8, pp. 1218–1233, Aug. 2002.
[15] M. Reyhanoglu, A. van der Schaft, N. H. McClamroch, and I. Kolmanovsky, "Dynamics and control of a class of underactuated mechanical systems," *IEEE Trans. Autom. Control*, vol. 44, no. 9, pp. 1663–1671, Sep. 1999.
[16] S. Sastry, *Nonlinear Systems: Analysis, Stability, and Control*. New York: Springer, 1999.
[17] M. W. Spong, "The swing up control problem for the Acrobot," *IEEE Control Syst. Mag.*, vol. 15, no. 1, pp. 49–55, Feb. 1995.
[18] M. W. Spong, "Energy based control of a class of underactuated mechanical systems," in *Proc. 1996 IFAC World Congr.*, vol. F, pp. 431–435.
[19] K. Suzuki, N. Kawai, T. Miyamoto, H. Tsuchiya, and S. Kimura, "Mechanics of kip motion," (in Japanese)*, Trans. Jpn Soc. Mech. Eng., C*, vol. 62, no. 10, pp. 241–246, 1996.
[20] V. A. Tsachouridis, "Robust control of a triple inverted pendulum," in *Proc. 1999 IEEE Int. Conf. Control Appl.*, vol. 2, pp. 1235–1240.
[21] X. Xin and M. Kaneda, "New analytical results of the energy based swinging up control of the Acrobot," in *Proc. 43rd IEEE Conf. Decis. Control*, 2004, pp. 704–709.
[22] X. Xin and M. Kaneda, "Analysis of the energy based swing-up control of the Acrobot," *Int. J. Robust Nonlinear Control*, vol. 17, no. 16, pp. 1503–1524, 2007.

Posture/Walking Control for Humanoid Robot Based on Kinematic Resolution of CoM Jacobian With Embedded Motion

Youngjin Choi, Doik Kim, Yonghwan Oh, and Bum-Jae You

***Abstract*—This paper proposes the walking pattern generation method, the kinematic resolution method of center of mass (CoM) Jacobian with embedded motions, and the design method of posture/walking controller for humanoid robots. First, the walking pattern is generated using the simplified model for bipedal robot. Second, the kinematic resolution of CoM Jacobian with embedded motions makes a humanoid robot balanced automatically during movement of all other limbs. Actually, it offers an ability of whole body coordination to humanoid robot. Third, the posture/walking controller is completed by adding the CoM controller minus the zero moment point controller to the suggested kinematic resolution method. We prove that the proposed posture/walking controller brings the disturbance input-to-state stability for the simplified bipedal walking robot model. Finally, the effectiveness of the suggested posture/walking control method is shown through experiments with regard to the arm dancing and walking of humanoid robot.**

***Index Terms*—Center of mass (CoM), CoM Jacobian, disturbance input-to-state stability (ISS), humanoid robot, posture/walking control, whole body coordination (WBC), zero moment point (ZMP).**

I. Introduction

Recently, there have been many researches about humanoid motion control, for example, walking control [1]–[6] and whole body coordination (WBC) [7]–[11]. Especially, the WBC algorithm with good performance becomes the essential part in the development of humanoid robot because it offers the enhanced stability and flexibility to the humanoid motion planning. In this paper, we suggest the kinematic resolution method of center of mass (CoM) Jacobian with embedded motion, which actually offers the ability of WBC to humanoid robot. For example, if humanoid robot stretches two arms forward, then the position of CoM of humanoid robot moves forward and its zero moment point (ZMP) swings back and forth. In this case, the proposed kinematic resolution method of CoM Jacobian with embedded (stretching arms) motion offers the joint configurations of supporting limb(s) calculated automatically to maintain the position of CoM fixed at one point.

Also, the walking controller design with good performance becomes an important part in the development of humanoid robot. In walking control, the ZMP control is the most important factor in implementing stable bipedal robot walking. If the ZMP is located in the convex region composed of outer contact points in sole(s) of support leg(s), then the robot will not at least fall down during walking. To implement the stable robot walking, the desired ZMP and CoM position planning methods were first suggested by using the inverted pendulum model and the fast Fourier transformation in [6]. Despite many references [1]–[6] to bipedal walking control methods, research on the stability of

Manuscript received January 8, 2007; revised May 25, 2007. This paper was recommended for publication by Associate Editor Q. Huang and Editor H. Arai upon evaluation of the reviewers' comments. This work was supported in part by the Information Technology Research and Development Program under Grant MIC and IITA 2006-S-028-01, and in part by the Bridge Inspection Robot Development Interface Program under Grant MOCT and KICTTEP, Korea. This paper was presented in part at the IEEE International Conference on Robotics and Automation (ICRA), Orlando, FL, May 2006.

Y. Choi is with the School of Electrical Engineering and Computer Science, Hanyang University, Ansan, 426-791, Korea (e-mail: cyj@hanyang.ac.kr).

D. Kim, Y. Oh, and B.-J. You are with Korea Institute of Science and Technology (KIST), Seoul, 136-791, Korea (e-mail: doikkim@kist.re.kr; oyh@kist.re.kr; ybj@kist.re.kr).

Digital Object Identifier 10.1109/TRO.2007.904907

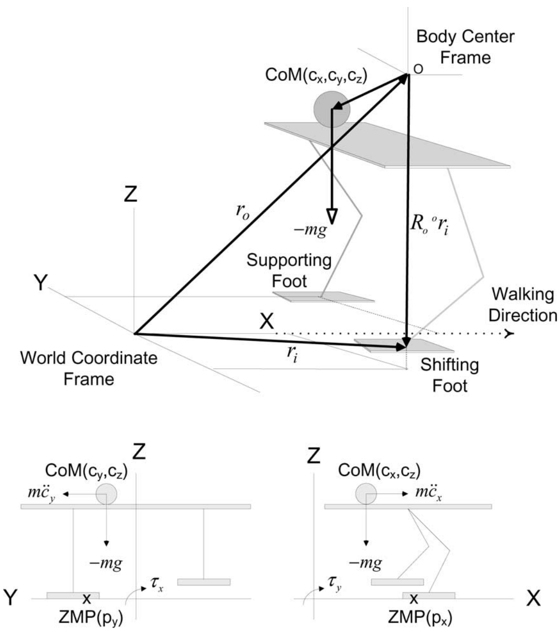

Fig. 1. Rolling Sphere Model for Dynamic Walking.

bipedal walking controllers is still lacking. In this paper, we propose the posture/walking control method and prove its disturbance input-to-state stability (ISS). The suggested method offers the stable robot walking as well as the function of WBC (or control) to humanoid robot.

This paper is organized as follows. Section II introduces a simplified model for bipedal walking robot. Section III proposes the walking pattern generation method by planning the desired CoM trajectory from the desired ZMP trajectory. Section IV explains the kinematic resolution method of CoM Jacobian with an embedded task or joint motion. Section V suggests the posture/walking controller for humanoid robot and proves its ISS for the simplified bipedal robot model. Section VI shows the experimental results about the stable robot walking and the WBC functions obtained by using the suggested kinematic resolution method of CoM Jacobian with embedded arm dancing motion. Section VII concludes the paper.

II. Simplified Model for Humanoid Robot

Since humanoid legs have high degrees of freedom for human-like walking, it is difficult to use their full dynamics to design the controller and to analyze the stability. Therefore, we will simplify the walking-related dynamics of bipedal robot as the equation of motion of a point mass concentrated on the position of CoM. This is obtained through the following procedures.

First, let us assume that the motion of CoM is constrained on the surface $z = c_z$, then the rolling sphere model with the concentrated point mass m can be obtained as the simplified model for bipedal robot, as shown in Fig. 1. The motion of the rolling sphere on a massless plate is described by the position of CoM $\boldsymbol{c} = [c_x, c_y, c_z]^T$ and the ZMP is described by the position on the ground $\boldsymbol{p} = [p_x, p_y, 0]^T$.

Second, let us take the moments about origin on the ground of the linear equations of motion for the rolling sphere (with a point mass = m) confined to motion on a plane $z = c_z$, as shown in Fig. 1, then the following equations are obtained:

$$\tau_x = mgc_y - m\ddot{c}_y c_z \tag{1}$$

$$\tau_y = -mgc_x + m\ddot{c}_x c_z \tag{2}$$

where g is the acceleration of gravity, c_z is the height constant of constraint plane, and τ_i is the moment about i-coordinate axis, for $i = x, y$. Now, if we introduce the conventional definition of ZMP as

$$p_x \triangleq -\frac{\tau_y}{mg} \quad \text{and} \quad p_y \triangleq \frac{\tau_x}{mg}$$

to (1) and (2), then ZMP equations can be obtained as two differential equations

$$p_x = c_x - \left(1/\omega_n^2\right)\ddot{c}_x \tag{3}$$

$$p_y = c_y - \left(1/\omega_n^2\right)\ddot{c}_y \tag{4}$$

where $\omega_n \triangleq \sqrt{g/c_z}$ is the natural radian frequency of the simplified biped walking robot system, and the value of ω_n is inversely proportional to the time that the CoM takes to fall to the ground. Actually, the aforementioned equations can be obtained easily by finding the position of zero moment on the ground in Fig. 1.

III. Desired ZMP/CoM Trajectories

In order to implement robot walking, first of all, the stepping positions on the ground and the support phases are predetermined. The stepping positions are generally represented as periodic functions with respect to time, and the support phases (double support and single support) are used in moving the ZMP. In a single support phase, the ZMP should stay in the footprint of supporting leg while the shifting leg is making a step. In a double support phase, the ZMP should be moved to the footprint region made by landing the shifting leg on the ground. These procedures should be repeated to make stable robot walking. The desired ZMP trajectory on the ground can be decomposed into X-directional and Y-directional piecewise continuous functions with respect to time. These will be explained in the following sections.

A. X-Directional Desired CoM Trajectory

The X-directional ZMP trajectory in Fig. 2 can be expressed by the function with respect to time, with a half period time T, as

$$p_x(t) = \begin{cases} (K_x/t_d)t, & \text{for} \quad 0 \le t \le t_d \\ B, & \text{for} \quad t_d < t < T - t_d \\ (2B - K_x) + (K_x/t_d)(t - (T - t_d)), & \\ & \text{for } T - t_d \le t \le T \end{cases} \tag{5}$$

where B is the constant that means the half of step length, and t_d means the time satisfying $p_x(t_d) = K_x$, namely, the change time from the double support phase to single support one. Also, positive B means the forward movement of CoM and negative B means the backward movement of CoM. Here, the desired CoM trajectory should be determined by solving (3) with the conditions of (5). We should notice that the X-directional ZMP trajectory is a piecewise continuous function with respect to time because it has the step discontinuities as shown in Fig. 2. However, the desired CoM trajectory should be obtained as the form of continuous function because the desired CoM motion is resolved kinematically according to the driving joint axis of the actuation motor in humanoid robot. First, during the double support time, the desired CoM trajectory becomes exactly equal to the desired ZMP trajectory because the linear CoM trajectory, with respect to time, defined as

$$c_x(t) \triangleq p_x(t), \quad \text{for} \quad 0 \le t \le t_d \quad \text{and} \quad T - t_d \le t \le T$$

satisfies the differential equation (3).

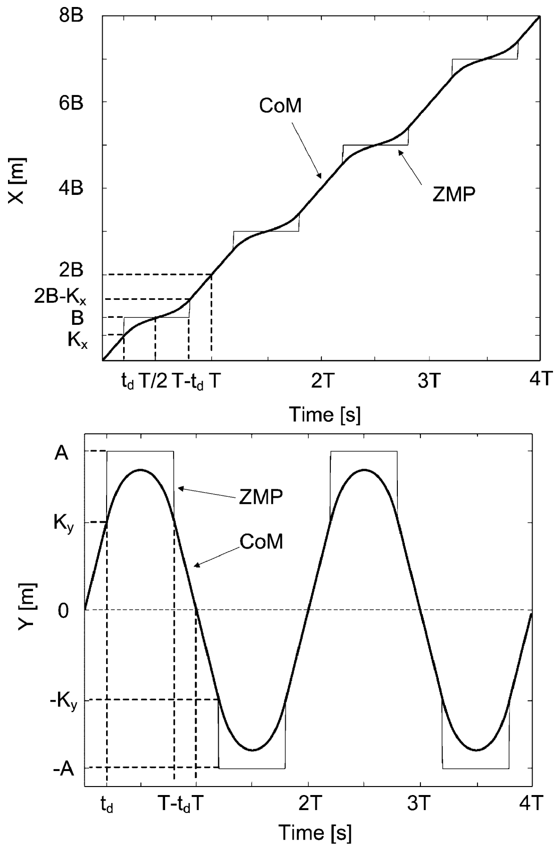

Fig. 2. Desired X- and Y-directional ZMP/CoM trajectories.

Second, during the single support time, we should solve the following differential equation:

$$\ddot{c}_x - \omega_n^2 c_x = -\omega_n^2 B, \quad \text{for } t_d < t < T - t_d. \tag{6}$$

In this case, the general solution is obtained as:

$$c_x(t) = C_{x1} \cosh(\omega_n (t - t_d)) + C_{x2} \sinh(\omega_n (t - t_d)) + B \tag{7}$$

with the coefficients C_{x1} and C_{x2}. For the continuity of CoM trajectory, the coefficients should satisfy the initial conditions

$$c_x(t_d) = K_x \quad \text{and} \quad \dot{c}_x(t_d) = K_x/t_d \tag{8}$$

and terminal conditions

$$c_x(T - t_d) = 2B - K_x \quad \text{and} \quad \dot{c}_x(T - t_d) = K_x/t_d. \tag{9}$$

Actually, for given constants B, ω_n, and T, we have four unknowns C_{x1}, C_{x2}, K_x, and t_d with aforementioned four conditions. From the initial conditions (8), we can get the following relations

$$C_{x1} = K_x - B \quad \text{and} \quad C_{x2} = \frac{K_x}{t_d \omega_n}. \tag{10}$$

Also, the terminal conditions (9) bring the same constraint as follows:

$$K_x = \frac{B t_d \omega_n}{t_d \omega_n + \tanh(\omega_n (T/2 - t_d))}. \tag{11}$$

In order to obtain a continuous desired CoM trajectory as shown in Fig. 2, three constraints mentioned earlier in (10) and (11) have to be satisfied only for a given piecewise continuous desired ZMP trajectory with respect to time.

B. Y-Directional Desired CoM Trajectory

The Y-directional ZMP trajectory in Fig. 2 can also be expressed by the function with respect to time as follow:

$$p_y(t) = \begin{cases} (K_y/t_d)t, & \text{for} \quad 0 \le t \le t_d \\ A, & \text{for} \quad t_d < t < T - t_d \\ (K_y/t_d)(T - t), & \text{for} \quad T - t_d \le t \le T \end{cases} \tag{12}$$

where A is the half of the distance between the center of left foot and that of the right foot. The positive constant A means that the first step is made by the right foot and the negative A means that the first step is by the left foot. As explained in previous section, $p_y(t_d) = K_y$ should be satisfied at the phase change time as shown in Fig. 2. Now, the continuous desired CoM trajectory can be determined by solving (4) with the conditions of (12). First, during the double support time, the desired CoM trajectory becomes exactly equal to the desired ZMP trajectory because the linear CoM trajectory, with respect to time, defined as follows:

$$c_y(t) \triangleq p_y(t), \quad \text{for } 0 \le t \le t_d \quad \text{and} \quad T - t_d \le t \le T$$

satisfies the differential equation (4).

Second, during the single support time, we should solve the following differential equation:

$$\ddot{c}_y - \omega_n^2 c_y = -\omega_n^2 A, \quad \text{for} \quad t_d < t < T - t_d. \tag{13}$$

The general solution is obtained as

$$c_y(t) = C_{y1} \cosh(\omega_n (t - t_d)) + C_{y2} \sinh(\omega_n (t - t_d)) + A \tag{14}$$

with the coefficients C_{y1} and C_{y2}. For the continuity of CoM trajectory, the coefficients should satisfy the initial conditions

$$c_y(t_d) = K_y \quad \text{and} \quad \dot{c}_y(t_d) = K_y/t_d \tag{15}$$

and the terminal conditions

$$c_y(T - t_d) = K_y \quad \text{and} \quad \dot{c}_y(T - t_d) = -K_y/t_d. \tag{16}$$

Actually, for given constants A, ω_n, and T, we have four unknowns C_{y1}, C_{y2}, K_y, and t_d with aforementioned four conditions. From the initial conditions (15), we can get the following relations:

$$C_{y1} = K_y - A \quad \text{and} \quad C_{y2} = \frac{K_y}{t_d \omega_n}. \tag{17}$$

Similar to the previous section, the terminal conditions (16) bring the same constraint as follows:

$$K_y = \frac{A t_d \omega_n \tanh(\omega_n (T/2 - t_d))}{1 + t_d \omega_n \tanh(\omega_n (T/2 - t_d))}. \tag{18}$$

In order to obtain a continuous desired CoM trajectory as shown in Fig. 2, three constraints in (17) and (18) mentioned before have to be satisfied only for given a piecewise continuous desired ZMP trajectory with respect to time.

For given walking constant parameters such as the natural radian frequency ω_n, the half period time T, the half distance of both feet A and the half step length B, if we determine the change time t_d of support phases, then the K_x and K_y are determined from (11) and (18), respectively, and then, the coefficients C_{x1}, C_{x2}, C_{y1}, and C_{y2} are determined from (10) and (17), respectively. As a result, the desired X-directional and Y-directional CoM trajectories can be obtained as forms of continuous functions as shown in Fig. 2. Actually, the support phase change times t_d and $T - t_d$ mean the takeoff time and the landing time of shifting foot, respectively. In order to implement the continuous desired CoM motions as shown in Fig. 2, the CoM inverse kinematics is required to resolve them kinematically according to the driving motor axes in humanoid robot. That is derived from the CoM Jacobian between the velocities of CoM and the joint velocities of all limbs. The concrete resolution method will be explained in the following section.

IV. Kinematic Resolution of CoM Jacobian with Embedded Motion

In this section, we will explain the kinematic resolution method of CoM Jacobian with embedded motion. Let a robot has n limbs and the first limb be the base limb, for example, $n = 4$ for humanoid robot except the neck. The base limb can be any limb but it should be on the ground to support the body. Each limb of a robot is hereafter considered as an independent limb. In general, the ith limb has the relation

$$ {}^{o}\dot{\boldsymbol{x}}_i = {}^{o}\boldsymbol{J}_i \dot{\boldsymbol{q}}_i \tag{19}$$

for $i = 1, 2, \ldots, n$, where ${}^{o}\dot{\boldsymbol{x}}_i \in \Re^6$ is the velocity of the end point of the ith limb, $\dot{\boldsymbol{q}}_i \in \Re^{n_i}$ is the joint velocity of the ith limb, ${}^{o}\boldsymbol{J}_i \in \Re^{6\times n_i}$ is the usual Jacobian matrix of the ith limb, and n_i means the number of active links of the ith limb. In order to realize the suggested robot walking, the number of active links of each leg should be at least six or more, namely, $n_i \geq 6$ for the leg limbs. The leading superscript o implies that the elements are represented on the body center coordinate system shown in Fig. 1, which is fixed on a humanoid robot.

A. Compatibility Condition

In our case, the body center is floating, and thus, the end point motion of the ith limb about the world coordinate system is written as

$$\dot{\boldsymbol{x}}_i = \boldsymbol{X}_i^{-1}\dot{\boldsymbol{x}}_o + \boldsymbol{X}_o {}^{o}\boldsymbol{J}_i \dot{\boldsymbol{q}}_i \tag{20}$$

where $\dot{\boldsymbol{x}}_o = [\dot{\boldsymbol{r}}_o^T; \boldsymbol{\omega}_o{}^T]^T \in \Re^6$ is the velocity of the body center represented on the world coordinate system, and

$$\boldsymbol{X}_i = \begin{bmatrix} \boldsymbol{I}_3 & [\boldsymbol{R}_o {}^{o}\boldsymbol{r}_i \times] \\ \boldsymbol{0}_3 & \boldsymbol{I}_3 \end{bmatrix} \quad \text{and} \quad \boldsymbol{X}_o = \begin{bmatrix} \boldsymbol{R}_o & \boldsymbol{0}_3 \\ \boldsymbol{0}_3 & \boldsymbol{R}_o \end{bmatrix}$$

where $\boldsymbol{X}_i$ is a (6×6) matrix that relates the body center velocity and the ith limb velocity, and $\boldsymbol{I}_3$ and $\boldsymbol{0}_3$ are an (3×3) identity and zero matrix, respectively. $\boldsymbol{R}_o {}^{o}\boldsymbol{r}_i$ is the position vector from the body center to the end point of the ith limb represented on the world coordinate frame and $[(\cdot)\times]$ is a skew-symmetric matrix for the cross product. Also, $\boldsymbol{X}_o$ is the transformation matrix, in which $\boldsymbol{R}_o \in \Re^{3\times 3}$ is the orientation of the body center represented on the world coordinate frame, and hereafter, we will use the relation $\boldsymbol{J}_i \triangleq \boldsymbol{X}_o {}^{o}\boldsymbol{J}_i$. Also, the concrete proof of (20) is in Appendix A.

All the limbs in a robot should have the same body center velocity, in other words, from (20), we can see that all the limbs should satisfy the compatibility condition that the body center velocity is the same, and thus, the ith limb and the jth limb should satisfy the following relation

$$\boldsymbol{X}_i(\dot{\boldsymbol{x}}_i - \boldsymbol{J}_i\dot{\boldsymbol{q}}_i) = \boldsymbol{X}_j(\dot{\boldsymbol{x}}_j - \boldsymbol{J}_j\dot{\boldsymbol{q}}_j). \tag{21}$$

From (21), the joint velocity of any limb can be represented by the joint velocity of the base limb and cartesian motions of limbs. Actually, the base limb should be chosen to be the support leg in single support phase or one of both legs in double support phase. Let us express the base limb with the subscript 1, then the joint velocity of the ith limb is expressed as

$$\dot{\boldsymbol{q}}_i = \boldsymbol{J}_i^+\dot{\boldsymbol{x}}_i - \boldsymbol{J}_i^+\boldsymbol{X}_{i1}(\dot{\boldsymbol{x}}_1 - \boldsymbol{J}_1\dot{\boldsymbol{q}}_1), \quad \text{for } i = 2, \ldots, n \tag{22}$$

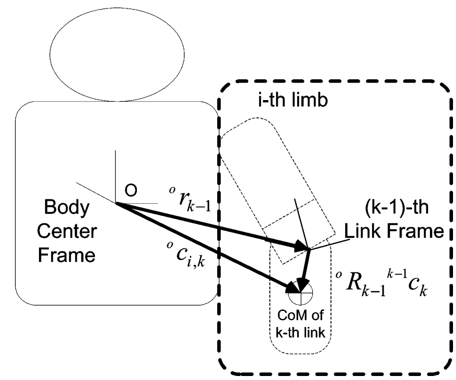

Fig. 3. Position of CoM of the kth link in the ith Limb: ${}^{o}\boldsymbol{c}_{i,k}$.

where $\boldsymbol{J}_i^+$ means the Moore–Penrose pseudoinverse of $\boldsymbol{J}_i$ and

$$\boldsymbol{X}_{i1} \triangleq \boldsymbol{X}_i^{-1}\boldsymbol{X}_1 = \begin{bmatrix} \boldsymbol{I}_3 & [\boldsymbol{R}_o({}^{o}\boldsymbol{r}_1 - {}^{o}\boldsymbol{r}_i)\times] \\ \boldsymbol{0}_3 & \boldsymbol{I}_3 \end{bmatrix}.$$

With this compatibility condition, the inverse kinematics of humanoid robot can be solved by using the information of base limb like (22), not by using the information of body center like (20).

B. CoM Jacobian With Fully Specified Embedded Motions

The position of CoM represented on the world coordinate frame, (see Fig. 1), is given by

$$\boldsymbol{c} = \boldsymbol{r}_o + \sum_{i=1}^{n} \boldsymbol{R}_o {}^{o}\boldsymbol{c}_i \tag{23}$$

where n is the number of limbs, $\boldsymbol{c}$ is the position vector of CoM represented on the world coordinate system, and ${}^{o}\boldsymbol{c}_i$ means the CoM position vector of the ith limb represented on the body center coordinate frame. Now, let us differentiate (23), then the conventional CoM Jacobian explained in [11] is obtained as

$$\dot{\boldsymbol{c}} = \dot{\boldsymbol{r}}_o + \boldsymbol{\omega}_o \times (\boldsymbol{c} - \boldsymbol{r}_o) + \sum_{i=1}^{n} \boldsymbol{R}_o {}^{o}\boldsymbol{J}_{c_i}\dot{\boldsymbol{q}}_i \tag{24}$$

where ${}^{o}\boldsymbol{J}_{c_i} \in \Re^{3\times n_i}$ means CoM Jacobian matrix of ith limb represented on the body center coordinate frame, n_i is the number of active links of the ith limb, and hereafter, we will use the relation $\boldsymbol{J}_{c_i} \triangleq \boldsymbol{R}_o {}^{o}\boldsymbol{J}_{c_i}$.

Remark 1: The CoM Jacobian matrix of the ith limb represented on the body center frame is expressed by

$${}^{o}\boldsymbol{J}_{c_i} \triangleq \sum_{k=1}^{n_i} \mu_{i,k} \frac{\partial {}^{o}\boldsymbol{c}_{i,k}}{\partial \boldsymbol{q}_i} \tag{25}$$

where ${}^{o}\boldsymbol{c}_{i,k} \in \Re^3$ means the position vector of center of mass of the kth link in ith limb represented on the body center frame as shown in Fig. 3 and the mass influence coefficient of the kth link in the ith limb is defined as

$$\mu_{i,k} \triangleq \frac{m_{i,k}}{\sum_{i=1}^{n}\sum_{k=1}^{n_i} m_{i,k}} = \frac{\text{mass of } k\text{th link in } i\text{th limb}}{\text{total mass}} \tag{26}$$

where the CoM position of the ith limb represented on body center frame is obtained as follows:

$${}^{o}\boldsymbol{c}_i = \sum_{k=1}^{n_i} \mu_{i,k} {}^{o}\boldsymbol{c}_{i,k}. \tag{27}$$

Also, the systematic derivation of CoM Jacobian matrix of (25) is given in Appendix B.

The motion of body center frame can be obtained by using (20) for the base limb as

$$\dot{\boldsymbol{x}}_o = \boldsymbol{X}_1 \{\dot{\boldsymbol{x}}_1 - \boldsymbol{J}_1 \dot{\boldsymbol{q}}_1\}$$
$$\begin{bmatrix} \dot{\boldsymbol{r}}_o \\ \boldsymbol{\omega}_o \end{bmatrix} = \begin{bmatrix} \boldsymbol{I}_3 & [\boldsymbol{R}_o {}^o\boldsymbol{r}_1 \times] \\ \boldsymbol{0}_3 & \boldsymbol{I}_3 \end{bmatrix} \left\{ \begin{bmatrix} \dot{\boldsymbol{r}}_1 \\ \boldsymbol{\omega}_1 \end{bmatrix} - \begin{bmatrix} \boldsymbol{J}_{v_1} \\ \boldsymbol{J}_{\omega_1} \end{bmatrix} \dot{\boldsymbol{q}}_1 \right\} \quad (28)$$

where $\boldsymbol{J}_{v_1}$ and $\boldsymbol{J}_{\omega_1}$ are the linear and angular velocity part of the base limb Jacobian $\boldsymbol{J}_1$ expressed on the world coordinate frame, respectively. Now, if (22) is applied to (24) for all limbs except the base limb with subscript 1, the CoM motion is rearranged as follows:

$$\dot{\boldsymbol{c}} = \dot{\boldsymbol{r}}_o + \boldsymbol{\omega}_o \times (\boldsymbol{c} - \boldsymbol{r}_o) + \boldsymbol{J}_{c_1} \dot{\boldsymbol{q}}_1 + \sum_{i=2}^{n} \boldsymbol{J}_{c_i} \boldsymbol{J}_i^+ (\dot{\boldsymbol{x}}_i - \boldsymbol{X}_{i1} \dot{\boldsymbol{x}}_1) + \sum_{i=2}^{n} \boldsymbol{J}_{c_i} \boldsymbol{J}_i^+ \boldsymbol{X}_{i1} \boldsymbol{J}_1 \dot{\boldsymbol{q}}_1. \quad (29)$$

Here, if (28) is applied to (29), then the CoM motion is only related with the motion of base limb

$$\dot{\boldsymbol{c}} = \dot{\boldsymbol{r}}_1 + \boldsymbol{\omega}_1 \times \boldsymbol{r}_{c1} - \boldsymbol{J}_{v_1} \dot{\boldsymbol{q}}_1 + \boldsymbol{r}_{c1} \times \boldsymbol{J}_{\omega_1} \dot{\boldsymbol{q}}_1 + \boldsymbol{J}_{c_1} \dot{\boldsymbol{q}}_1 + \sum_{i=2}^{n} \boldsymbol{J}_{c_i} \boldsymbol{J}_i^+ (\dot{\boldsymbol{x}}_i - \boldsymbol{X}_{i1} \dot{\boldsymbol{x}}_1) + \sum_{i=2}^{n} \boldsymbol{J}_{c_i} \boldsymbol{J}_i^+ \boldsymbol{X}_{i1} \boldsymbol{J}_1 \dot{\boldsymbol{q}}_1 \quad (30)$$

where $\boldsymbol{r}_{c1} = \boldsymbol{c} - \boldsymbol{r}_1$. Also, if the base limb has the face contact with the ground (the end point of base limb represented on world coordinate frame is fixed, $\dot{\boldsymbol{x}}_1 = \boldsymbol{0}$, namely, $\dot{\boldsymbol{r}}_1 = \boldsymbol{0}, \boldsymbol{\omega}_1 = \boldsymbol{0}$), then the CoM Jacobian matrix with fully specified embedded motions can be written like usual kinematic Jacobian of base limb

$$\dot{\boldsymbol{c}}_{\mathrm{fsem}} = \boldsymbol{J}_{\mathrm{fsem}}\, \dot{\boldsymbol{q}}_1 \quad (31)$$

where

$$\dot{\boldsymbol{c}}_{\mathrm{fsem}} \triangleq \dot{\boldsymbol{c}} - \sum_{i=2}^{n} \boldsymbol{J}_{c_i} \boldsymbol{J}_i^+ \dot{\boldsymbol{x}}_i \quad (32)$$

$$\boldsymbol{J}_{\mathrm{fsem}} \triangleq -\boldsymbol{J}_{v_1} + \boldsymbol{r}_{c1} \times \boldsymbol{J}_{\omega_1} + \boldsymbol{J}_{c_1} + \sum_{i=2}^{n} \boldsymbol{J}_{c_i} \boldsymbol{J}_i^+ \boldsymbol{X}_{i1} \boldsymbol{J}_1. \quad (33)$$

Here, if the CoM Jacobian with fully specified embedded motions is augmented with the orientation Jacobian of body center ($\boldsymbol{\omega}_o = -\boldsymbol{J}_{\omega_1} \boldsymbol{q}_1$) and all desired cartesian motions are embedded in (32), then the desired joint configurations of base limb (support limb) are resolved as

$$\dot{\boldsymbol{q}}_{1,d} = \begin{bmatrix} \boldsymbol{J}_{\mathrm{fsem}} \\ -\boldsymbol{J}_{\omega_1} \end{bmatrix}^+ \begin{bmatrix} \dot{\boldsymbol{c}}_{\mathrm{fsem},d} \\ \boldsymbol{\omega}_{o,d} \end{bmatrix} \quad (34)$$

where the subscript d means the desired motion and

$$\dot{\boldsymbol{c}}_{\mathrm{fsem},d} = \dot{\boldsymbol{c}}_d - \textstyle\sum_{i=2}^{n} \boldsymbol{J}_{c_i} \boldsymbol{J}_i^+ \dot{\boldsymbol{x}}_{i,d}. \quad (35)$$

The CoM motion with fully specified embedded motions $\dot{\boldsymbol{c}}_{\mathrm{fsem},d}$ consists of two relations: a given desired CoM motion (the first term) described in the previous section and the relative effect of other limbs (the second term), in which all the given desired limb motions $\dot{\boldsymbol{x}}_{i,d}$ are embedded in the relation of CoM Jacobian, thus, the effect of the CoM movement generated by the given limb motion is compensated by the base limb. By solving (34), the desired joint motion of the base limb is obtained. The resulting base limb motion makes a humanoid robot balanced automatically during the movement of the all other limbs. With the desired joint motion of base limb, the desired joint motions of all other limbs can be obtained by (22) as follows:

$$\dot{\boldsymbol{q}}_{i,d} = \boldsymbol{J}_i^+ (\dot{\boldsymbol{x}}_{i,d} + \boldsymbol{X}_{i1} \boldsymbol{J}_1 \dot{\boldsymbol{q}}_{1,d}), \quad \text{for } i = 2, \ldots, n. \quad (36)$$

The resulting motion follows the given desired motions, regardless of balancing motion by base limb. In other words, the suggested kinematic resolution method of CoM Jacobian with embedded motion offers the WBC function to the humanoid robot automatically.

C. CoM Jacobian With Partially Specified Embedded Motion

In some cases, the desired motion of any limb is specified in the joint configuration space. For example, let us consider that the walking motions (for the leg limbs of $i = 1, 2$) are partially specified in cartesian space and the other limb motions (for $i = 3, \ldots, n$) in joint space, then the CoM Jacobian of (31) in the previous section should be slightly modified and its kinematic resolution method should also be modified as

$$\dot{\boldsymbol{q}}_{1,d} = \begin{bmatrix} \boldsymbol{J}_{\mathrm{psem}} \\ -\boldsymbol{J}_{\omega_1} \end{bmatrix}^+ \begin{bmatrix} \dot{\boldsymbol{c}}_{\mathrm{psem},d} \\ \boldsymbol{\omega}_{o,d} \end{bmatrix} \quad (37)$$

$$\dot{\boldsymbol{q}}_{2,d} = \boldsymbol{J}_2^+ (\dot{\boldsymbol{x}}_{2,d} + \boldsymbol{X}_{21} \boldsymbol{J}_1 \dot{\boldsymbol{q}}_{1,d}) \quad (38)$$

where the CoM desired motion and CoM Jacobian with partially specified embedded motion are respectively, expressed by

$$\dot{\boldsymbol{c}}_{\mathrm{psem},d} \triangleq \dot{\boldsymbol{c}}_d - \boldsymbol{J}_{c_2} \boldsymbol{J}_2^+ \dot{\boldsymbol{x}}_{2,d} - \sum_{i=3}^{n} \boldsymbol{J}_{c_i} \dot{\boldsymbol{q}}_{i,d} \quad (39)$$

$$\boldsymbol{J}_{\mathrm{psem}} \triangleq -\boldsymbol{J}_{v_1} + \boldsymbol{r}_{c1} \times \boldsymbol{J}_{\omega_1} + \boldsymbol{J}_{c_1} + \boldsymbol{J}_{c_2} \boldsymbol{J}_2^+ \boldsymbol{X}_{21} \boldsymbol{J}_1. \quad (40)$$

For example, in order to implement only the robot walking by using CoM Jacobian with partially specified embedded motion, the desired motions of other limbs except leg limbs should be zero, namely, $\dot{\boldsymbol{q}}_{i,d} = \boldsymbol{0}$ for $i = 3, \ldots, n$ in (39). In this case, the desired joint configurations of first (base) limb can be obtained by solving (37) and then, those of second limb by (38). On the other hand, if we are to implement only the robot arm dancing motion with zero CoM motion, then the desired dancing arm motions, namely, $\dot{\boldsymbol{q}}_{i,d}$ for $i = 3, \ldots, n$, and $\dot{\boldsymbol{c}}_d = \boldsymbol{0}, \dot{\boldsymbol{x}}_{2,d} = \boldsymbol{0}$ in (39), are embedded in the suggested resolution method of (37) and (38). In many cases, the motion of base limb (support leg) are automatically generated with the function of autobalancing. This is the main advantage of the proposed method.

V. Stability of Posture/Walking Controller

Since a humanoid robot is an electromechanical system including many electric motors, gears, and link mechanisms, there exist many disturbances in implementing the desired motions of CoM and ZMP with a real bipedal robot system. To show the robustness of the controller to be suggested against disturbances, we apply the following stability theory to a bipedal robot control system. The control system is said to be disturbance ISS [12], if there exists a smooth positive definite radially unbounded function $V(\boldsymbol{e}, t)$, a class $\mathcal{K}_\infty$ function γ_1, and a class $\mathcal{K}$ function γ_2 such that the following dissipativity inequality is satisfied

$$\dot{V} \le -\gamma_1(|\boldsymbol{e}|) + \gamma_2(|\boldsymbol{\epsilon}|) \quad (41)$$

where $\boldsymbol{e}$ is the error state vector and $\boldsymbol{\epsilon}$ is the disturbance input vector. In this section, we propose the posture/walking controller for bipedal robot systems as shown in Fig. 4. In this figure, first, the ZMP planer and CoM planer generate the desired trajectories in Fig. 2 satisfying the following differential equation

$$p_{i,d} = c_{i,d} - 1/\omega_n^2 \ddot{c}_{i,d}, \quad \text{for } i = x, y. \quad (42)$$

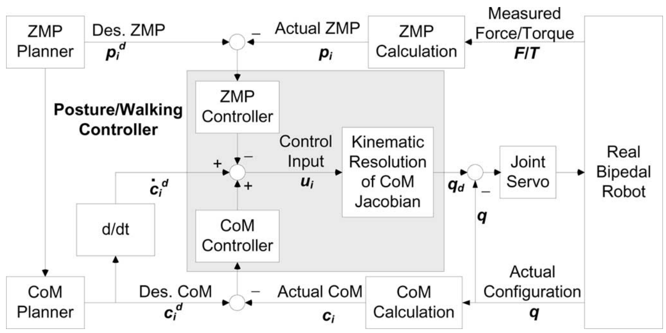

Fig. 4. Posture/Walking Controller for Humanoid Robot.

Second, the simplified model for the real bipedal walking robot has the following dynamics

$$\dot{c}_i = u_i + \epsilon_i$$
$$p_i = c_i - 1/\omega_n^2 \ddot{c}_i, \quad \text{for } i = x, y \tag{43}$$

where ϵ_i is the disturbance input produced by actual control error, u_i is the control input, c_i and p_i are the actual positions of CoM and ZMP measured from the real bipedal robot, respectively. Actually, the real bipedal robot offers the ZMP information from force/torque sensors attached to the ankles of humanoid and the CoM information from the encoder data attached to the motor driving axes, respectively, as shown in Fig. 4. Here, we assume that the the disturbance produced by control error is bounded and its differentiation is also bounded, namely, $|\epsilon_i| < a$ and $|\dot{\epsilon}_i| > b$ with some positive constants a and b. The following theorem proves the stability of the posture/walking controller for the simplified walking robot model.

Theorem 1: Let us define the ZMP and CoM errors for the simplified bipedal robot control system (43) as follows:

$$e_{p,i} \triangleq p_{i,d} - p_i \quad \text{and} \quad e_{c,i} \triangleq c_{i,d} - c_i, \quad \text{for } i = x, y.$$

If the control input u_i in Fig. 4 has the form

$$u_i = \dot{c}_i^d - k_{p,i} e_{p,i} + k_{c,i} e_{c,i} \tag{44}$$

under the gain conditions

$$k_{c,i} > \omega_n > 1 \quad \text{and} \quad 0 < k_{p,i} < \omega_n - (\beta^2/\omega_n) - \gamma^2 \tag{45}$$

with any positive constants satisfying the conditions

$$\beta < \omega_n \quad \text{and} \quad \gamma < \sqrt{\omega_n - (\beta^2/\omega_n)}$$

then the posture/walking controller gives the disturbance input $(\epsilon_i, \dot{\epsilon}_i)$-to-state $(e_{p,i}, e_{c,i})$ stability to a simplified bipedal walking robot, where the $k_{p,i}$ is the proportional gain of ZMP controller and $k_{c,i}$ is that of CoM controller in Fig. 4.

Proof. For proof see [1].

To make active use of the suggested control scheme, the control input $\boldsymbol{u}$ of (44) suggested in Theorem 1 is applied to the place of the term $\dot{\boldsymbol{c}}_d$ in (35) or (39). In other words, (35) and (39) are modified to include the ZMP and CoM controllers as

$$\dot{\boldsymbol{c}}_{\mathrm{fsem},d} = \boldsymbol{u} - \sum_{i=2}^{n} \boldsymbol{J}_{c_i} \boldsymbol{J}_i^+ \dot{\boldsymbol{x}}_{i,d} \tag{46}$$

and

$$\dot{\boldsymbol{c}}_{\mathrm{psem},d} = \boldsymbol{u} - \boldsymbol{J}_{c_2} \boldsymbol{J}_2^+ \dot{\boldsymbol{x}}_{2,d} - \sum_{i=3}^{n} \boldsymbol{J}_{c_i} \dot{\boldsymbol{q}}_{i,d} \tag{47}$$

where $\boldsymbol{u} \triangleq \dot{\boldsymbol{c}}_d - \boldsymbol{k}_p \boldsymbol{e}_p + \boldsymbol{k}_c \boldsymbol{e}_c$, in which $\boldsymbol{u} = [u_x, u_y, u_z]^T$, $\boldsymbol{e}_p = [e_{p,x}, e_{p,y}, 0]^T$, $\boldsymbol{e}_c = [e_{c,x}, e_{c,y}, e_{c,z}]^T$, $\boldsymbol{k}_p$ and $\boldsymbol{k}_c$ imply the (3×3) diagonal gain matrices composed of the corresponding diagonal elements $\{k_{p,x}, k_{p,y}, 0\}$ and $\{k_{c,x}, k_{c,y}, k_{c,z}\}$, respectively. And then, the kinematic resolution methods suggested in previous section are utilized to obtain the desired joint motions of base limb and other limbs, as shown in Fig. 4.

Remark 2: Note that the ZMP controller in Theorem 1 has the positive feedback different from the conventional controller. Also, for practical use, the gain conditions of ZMP and CoM controller in the posture/walking control scheme can be simply rewritten without arbitrary positive constants β and γ as

$$k_{c,i} > \omega_n \quad \text{and} \quad 0 < k_{p,i} < \omega_n, \quad \text{for } i = x, y$$

because the stability proof is very conservative in Theorem 1.

As shown in Fig. 4, the suggested posture/walking control scheme can be divided as the kinematic resolution of CoM Jacobian with (fully specified or partially specified) embedded motion and ZMP/CoM control. The proposed kinematic resolution method has main advantage such that it offers the whole body coordination function such as balance control to humanoid robot automatically. Also, the proposed ZMP/CoM control methods offer the enhanced stability and robustness to humanoid motion control system against unknown disturbances.

VI. Experimental Results

In this section, we show the performance and robustness of proposed posture/walking control scheme through two experiments for humanoid robot "Mahru I" developed by Korea Institute of Science and Technology (KIST). The Denavit–Hartenberg parameters for kinematics and centroid/mass data for CoM kinematics are given in Table I. These data are utilized for the suggested kinematic resolution of CoM Jacobian with embedded motion.

For the forward walking experiment, the desired CoM trajectories suggested in previous section are used during first half period as follows:

$$c_{x,d}(t) = \begin{cases} (K_x/t_d)t, & \text{for } 0 \le t \le t_d \\ C_{x1}\cosh(\omega_n(t-t_d)) + C_{x2}\sinh(\omega_n(t-t_d)) + B, & \\ & \text{for } t_d < t < T - t_d \\ (2B - K_x) + (K_x/t_d)(t - (T - t_d)), & \\ & \text{for } T - t_d \le t \le T \end{cases}$$

$$c_{y,d}(t) = \begin{cases} (K_y/t_d)t, & \text{for } 0 \le t \le t_d \\ C_{y1}\cosh(\omega_n(t-t_d)) + C_{y2}\sinh(\omega_n(t-t_d)) + A, & \\ & \text{for } t_d < t < T - t_d \\ (K_y/t_d)(T - t), & \text{for } T - t_d \le t \le T \end{cases}$$

$$c_{z,d}(t) = c_z(0) \quad \text{(as initial value)}$$
$$\boldsymbol{\omega}_{o,d}(t) = \boldsymbol{0}. \tag{48}$$

Also, the desired motion of second limb ($\dot{\boldsymbol{x}}_{2,d} = [\dot{\boldsymbol{r}}_{2,d}^T; \boldsymbol{\omega}_{2,d}^T]^T$) for the forward walking can be set during first half period as

$$r_{2,x,d}(t) = \begin{cases} 0, & \text{for } 0 \le t \le t_d \\ B[\sin(\omega_r(t - t_d) - \pi/2) + 1], & \\ & \text{for } t_d < t < T - t_d \\ 2B, & \text{for } T - t_d \le t \le T \end{cases}$$

$$r_{2,y,d}(t) = -A$$

TABLE I
THE DH PARAMETERS, CENTROID AND MASS DATA OF KIST "MAHRU I"

Left Leg	α (rad)	a (m)	d (m)	θ (rad)	centroid (σ_x, σ_y, σ_z) (m)	mass (kg)
LL0	0	0.09	-0.146	$\pi/2$	(0.0,0.031,-0.0338)	2.067
1	$\pi/2$	0	0	0	(0.0295,0.0,-0.0015)	1.8206
2	$\pi/2$	0	0	$-\pi/2$	(0.2249,0.0187,-0.0156)	3.3586
3	0	0.31	0	0	(0.1451,0.0285,-0.0026)	2.2238
4	0	0.31	0	0	(0.0,-0.0257,-0.0143)	2.6922
5	$-\pi/2$	0	0	0	(0.0951,0.0047,0.0083)	1.9091
6	0	0.103	0	0	x	x
Right Leg						
RL0	0	-0.09	-0.146	$\pi/2$	(0.0,0.031,-0.0338)	2.067
1	$\pi/2$	0	0	0	(-0.0295,0.0,-0.0015)	1.8206
2	$\pi/2$	0	0	$-\pi/2$	(0.2249,0.0187,0.0156)	3.3586
3	0	0.31	0	0	(0.1451,0.0285,0.0026)	2.2238
4	0	0.31	0	0	(0.0,-0.0257,0.0143)	2.6922
5	$-\pi/2$	0	0	0	(0.0951,-0.0047,0.0083)	1.9091
6	0	0.103	0	0	x	x
Left Arm						
LA0	0	0	0	0	(0.0278,0.0,-0.051)	0.823
1	$-\pi/2$	0	-0.061	$-\pi/2$	(0.062,0.000125,-0.0085)	1.437
2	$\pi/2$	0	-0.0055	$\pi/2$	(0.00798,-0.00146,0.2)	0.9
3	$-\pi/2$	0	0.224	$\pi/2$	(0.0,-0.0228,0.00739)	0.11
4	$\pi/2$	0	0	0	(-0.0025,0.000035,0.153)	0.781
5	$-\pi/2$	0	0.225	$-\pi/2$	(0.0,-0.0208,0.017)	0.053
6	0	0.041	0	$-\pi/2$	x	x
Right Arm						
RA0	0	0	0	0	(0.0278,0.0,0.051)	0.823
1	$-\pi/2$	0	0.061	$-\pi/2$	(0.062,0.000125,-0.0085)	1.437
2	$\pi/2$	0	-0.0055	$\pi/2$	(-0.00798,-0.00146,0.2)	0.9
3	$-\pi/2$	0	0.224	$\pi/2$	(0.0,-0.0228,-0.00739)	0.11
4	$\pi/2$	0	0	0	(-0.0025,0.000035,0.153)	0.781
5	$-\pi/2$	0	0.225	$-\pi/2$	(0.0,-0.0208,0.017)	0.053
6	0	0.041	0	$-\pi/2$	x	x
Head						
H0	0	0.04	0.47	0	(0.0,0.0,0.0)	0.5
1	$-\pi/2$	0	0	0	(0.0,0.0,0.0)	0.5
2	0	0	0	0	x	x
Pelvis	x	x	x	x	(-0.056,0.0,-0.0173)	4.6341
Waist	x	x	x	x	(0.0,0.0,0.17)	25.7

$$r_{2,z,d}(t) = \begin{cases} 0, & \text{for} \quad 0 \le t \le t_d \\ h_o/2[\sin(2\omega_r(t-t_d) - \pi/2) + 1], & \\ & \text{for} \quad t_d < t < T - t_d \\ 0, & \text{for} \quad T - t_d \le t \le T \end{cases}$$
$$\boldsymbol{\omega}_{2,d}(t) = \mathbf{0} \tag{49}$$

where $\omega_r = \pi/(T - 2t_d)$ and h_o is the step height of second limb (swing leg). Also, as the support leg is switched between left leg and right leg, the base limb should also be switched according to the support phase of left/right leg in order to implement the walking motion as shown in Fig. 2. In other words, the left leg becomes the first (base) limb and the right leg is second limb during the first half period or for $0 \le p_x(t) < 2B$ in Fig. 2, and then, the right leg becomes the first (base) limb and left leg is second limb during the second half period or for $2B \le p_x(t) < 4B$ in Fig. 2, and later, the left leg becomes first (base) limb again. These procedures should be repeated to implement the walking motion.

We experimented the walking motions of (48) and (49) with the proposed posture/walking control scheme as shown in Fig. 4. The utilized parameters are as follows: the half period time $T = 1.0$ [s], the support change time $t_d = 0.1$ [s], half distance between both feet $A = 0.09$ [m], the half step length $B = 0.1$ [m], the total mass $m = 67.68$ [kg], the height constant of constraint surface $c_z = 0.687$ [m], the step height of shift leg $h_o = 0.04$ [m], the natural radian frequency $\omega_n = \sqrt{g/c_z} = 3.78$, and the gains of proposed ZMP/CoM controllers are set as $k_{p,i} = \{3.0, 1.8, 0.0\}$ and $k_{c,i} = \{6.6, 3.8, 3.2\}$ for $i = x, y, z$. The experimental results are shown in Fig. 5, which shows the X-directional and Y-directional experimental results about ZMP/CoM trajectories with respect to time, respectively. In spite of the disturbances caused by the contact forces/moments in the landing phase of swing leg, these experimental results demonstrate the robustness of proposed posture/walking controller while following the desired CoM and ZMP trajectories.

Second, in order to show the automatic balancing (or the function of WBC) by the posture/walking controller, we experimented the dancing

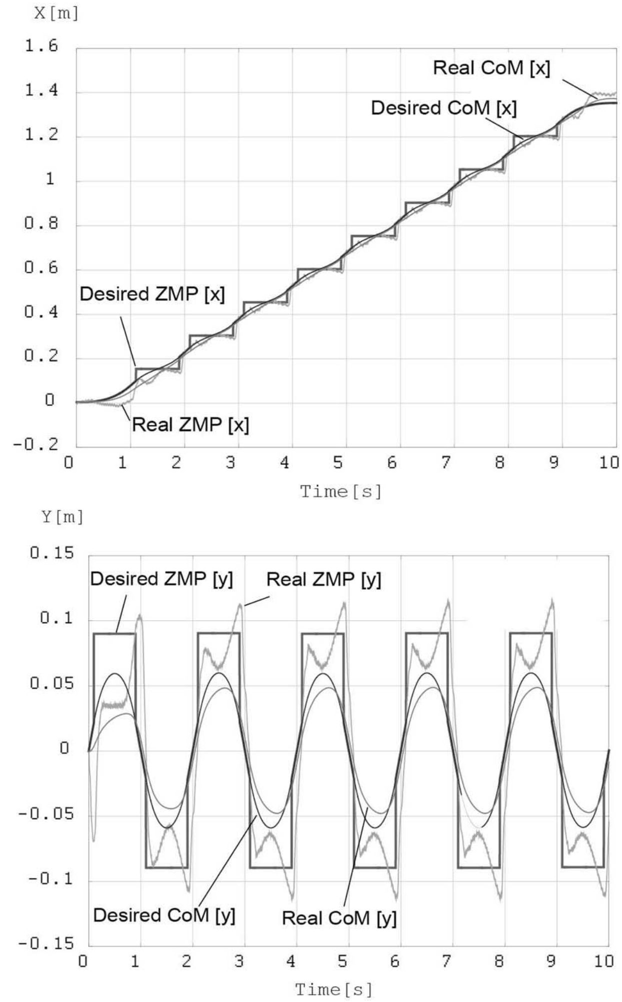

Fig. 5. Experimental result 1: desired and real CoM and ZMP trajectories while walking.

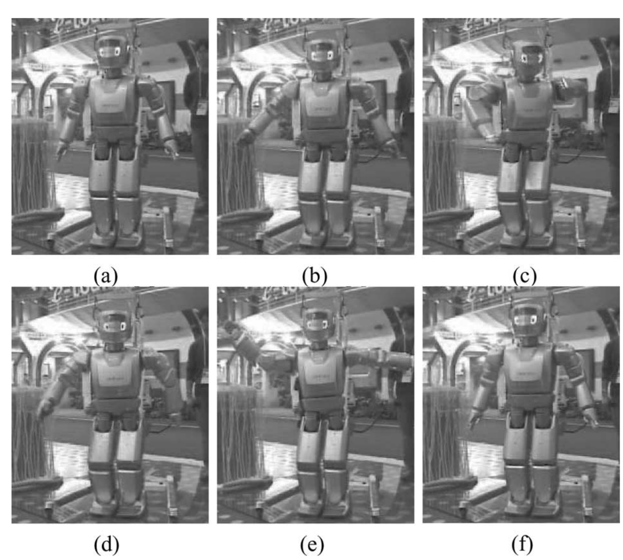

Fig. 6. Experimental result 2: snapshots while dancing. (a) 0 [s]. (b) 20 [s]. (c) 40 [s]. (d) 60 [s]. (e) 80 [s]. (f) Ending.

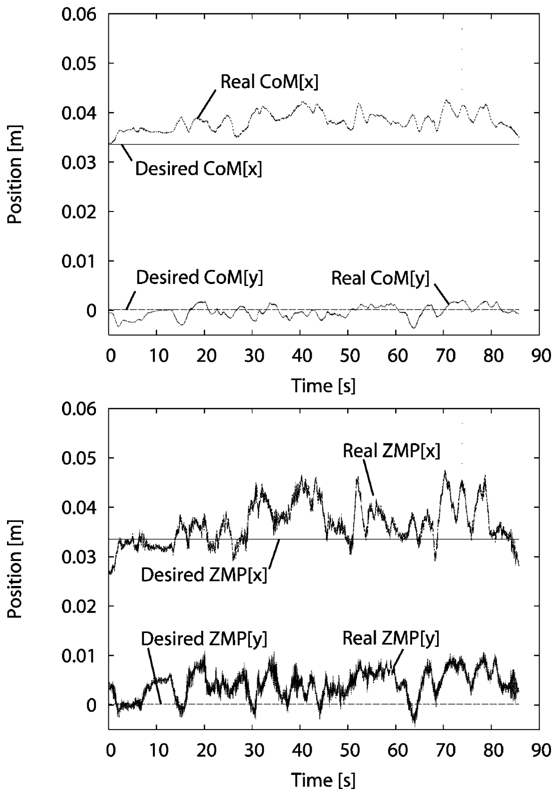

Fig. 7. Experimental result 2: desired and real CoM and ZMP while dancing.

arm motion of humanoid robot. The desired dancing arm motions are applied to the dual arms, then the support left/right legs motions are generated by using the posture/walking control scheme suggested in Fig. 4. Here, we utilized the kinematic resolution method of CoM Jacobian with the partially specified embedded motion, the partially specified embedded CoM motion term $\dot{\boldsymbol{c}}_{\mathrm{psem},d}$ is automatically changed with the desired dancing arm motions ($\dot{\boldsymbol{q}}_{3,d}$ and $\dot{\boldsymbol{q}}_{4,d}$) in (47), and then, both desired leg motions ($\dot{\boldsymbol{q}}_{1,d}$ and $\dot{\boldsymbol{q}}_{2,d}$) are generated by using (37) and (38). The experimental results are shown as snapshots according to time progress in Fig. 6. Though the joint configurations of dual arms are rapidly changed with the dancing arm motions, the ZMP and CoM positions are not nearly changed at the initial position, as shown in Fig. 7. The joint configurations of both legs are automatically generated to maintain the CoM position constantly. Also, we can see in Fig. 7 that the ZMP and CoM errors are within the bounds of ± 0.01 [m] approximately. As a result, we could succeed in implementing the fast dancing arm motion stably, thanks to the developed posture/walking control scheme.

VII. Conclusion

In this paper, the desired CoM/ZMP trajectory planning method, the kinematic resolution method of CoM Jacobian with embedded walking or dancing arm motion, and the design method of ZMP and CoM controller were proposed for humanoid robot. As a result, the proposed kinematic resolution method with CoM Jacobian offers the whole body coordination function to the humanoid robot automatically. Also, the disturbance ISS of the proposed ZMP/CoM controller was proved to show the robustness against disturbances. Finally, we showed the effectiveness of the proposed methods through experiments.

Appendix

A. Proof of (20)

In Fig. 1, the end-point position of the ith limb represented on the world coordinate is given by

$$\boldsymbol{r}_i = \boldsymbol{r}_o + \boldsymbol{R}_o {}^o\boldsymbol{r}_i$$

where $\boldsymbol{R}_o$ is the rotation matrix of body center frame with respect to world coordinate frame. Let us differentiate the aforementioned equation, then

$$\begin{aligned}
\dot{\boldsymbol{r}}_i &= \dot{\boldsymbol{r}}_o + \dot{\boldsymbol{R}}_o {}^o\boldsymbol{r}_i + \boldsymbol{R}_o {}^o\dot{\boldsymbol{r}}_i \leftarrow \dot{\boldsymbol{R}}_o = [\boldsymbol{\omega}_o \times]\boldsymbol{R}_o \\
\dot{\boldsymbol{r}}_i &= \dot{\boldsymbol{r}}_o + [\boldsymbol{\omega}_o \times]\boldsymbol{R}_o {}^o\boldsymbol{r}_i + \boldsymbol{R}_o {}^o\dot{\boldsymbol{r}}_i \leftarrow [\boldsymbol{a}\times]\boldsymbol{b} = -[\boldsymbol{b}\times]\boldsymbol{a} \\
\dot{\boldsymbol{r}}_i &= \dot{\boldsymbol{r}}_o - [\boldsymbol{R}_o {}^o\boldsymbol{r}_i \times]\boldsymbol{\omega}_o + \boldsymbol{R}_o {}^o\dot{\boldsymbol{r}}_i
\end{aligned}$$

in which

$$[\boldsymbol{a}\times] = \begin{bmatrix} 0 & -a_z & a_y \\ a_z & 0 & -a_x \\ -a_y & a_x & 0 \end{bmatrix}.$$

Now, if we include the angular velocity, then the total velocity of the ith limb motion represented on the world coordinate can be obtained as follows:

$$\begin{aligned}
\dot{\boldsymbol{r}}_i &= \dot{\boldsymbol{r}}_o - [\boldsymbol{R}_o {}^o\boldsymbol{r}_i \times]\boldsymbol{\omega}_o + \boldsymbol{R}_o {}^o\dot{\boldsymbol{r}}_i \\
\boldsymbol{\omega}_i &= \boldsymbol{\omega}_o + \boldsymbol{R}_o {}^o\boldsymbol{\omega}_i.
\end{aligned}$$

Therefore,

$$\begin{bmatrix} \dot{\boldsymbol{r}}_i \\ \boldsymbol{\omega}_i \end{bmatrix} = \begin{bmatrix} \boldsymbol{I}_3 & -[\boldsymbol{R}_o {}^o\boldsymbol{r}_i \times] \\ \boldsymbol{0}_3 & \boldsymbol{I}_3 \end{bmatrix} \begin{bmatrix} \dot{\boldsymbol{r}}_o \\ \boldsymbol{\omega}_o \end{bmatrix} + \begin{bmatrix} \boldsymbol{R}_o & \boldsymbol{0}_3 \\ \boldsymbol{0}_3 & \boldsymbol{R}_o \end{bmatrix} \begin{bmatrix} {}^o\dot{\boldsymbol{r}}_i \\ {}^o\boldsymbol{\omega}_i \end{bmatrix}$$

$$\begin{aligned}
&\text{in short} \quad \dot{\boldsymbol{x}}_i = \boldsymbol{X}_i^{-1}\dot{\boldsymbol{x}}_o + \boldsymbol{X}_o {}^o\dot{\boldsymbol{x}}_i \\
&\therefore \quad \dot{\boldsymbol{x}}_i = \boldsymbol{X}_i^{-1}\dot{\boldsymbol{x}}_o + \boldsymbol{X}_o {}^o\boldsymbol{J}_i\dot{\boldsymbol{q}}_i \ \leftarrow \ {}^o\dot{\boldsymbol{x}}_i = {}^o\boldsymbol{J}_i\dot{\boldsymbol{q}}_i.
\end{aligned}$$

B. Derivation of CoM Jacobian of ith limb : ${}^o\boldsymbol{J}_{c_i}$

In Fig. 3, the CoM position of kth link in ith limb represented on the body center frame is given by

$${}^o\boldsymbol{c}_{i,k} = {}^o\boldsymbol{r}_{k-1} + {}^o\boldsymbol{R}_{k-1} {}^{k-1}\boldsymbol{c}_k$$

where ${}^o\boldsymbol{r}_{k-1}$ and ${}^o\boldsymbol{R}_{k-1}$ mean the position and rotation matrix of the $(k-1)$th link frame coordinate in the ith limb represented on the body center frame; respectively, and

$${}^{k-1}\boldsymbol{c}_k \triangleq \boldsymbol{R}_z(q_k)\boldsymbol{\sigma}_k = \begin{bmatrix} \cos(q_k) & -\sin(q_k) & 0 \\ \sin(q_k) & \cos(q_k) & 0 \\ 0 & 0 & 1 \end{bmatrix} \begin{bmatrix} \sigma_{k,x} \\ \sigma_{k,y} \\ \sigma_{k,z} \end{bmatrix}$$

in which $\boldsymbol{R}_z(q_k)$ is the z-directional rotation matrix about the kth link driving axis and $\boldsymbol{\sigma}_k$ means the constant centroid position of the kth link with respect to $(k-1)$th frame; this should be obtained from the design procedures of robot similar to the Denavit–Hartenberg parameters. Let us differentiate and rearrange the aforementioned equation as

$$\begin{aligned}
{}^o\dot{\boldsymbol{c}}_{i,k} &= {}^o\dot{\boldsymbol{r}}_{k-1} + {}^o\dot{\boldsymbol{R}}_{k-1} {}^{k-1}\boldsymbol{c}_k + {}^o\boldsymbol{R}_{k-1} {}^{k-1}\dot{\boldsymbol{c}}_k \\
&= {}^o\dot{\boldsymbol{r}}_{k-1} + {}^o\boldsymbol{\omega}_{k-1} \times {}^o\boldsymbol{R}_{k-1} {}^{k-1}\boldsymbol{c}_k + {}^o\boldsymbol{R}_{k-1}({}^{k-1}\boldsymbol{\omega}_k \times {}^{k-1}\boldsymbol{c}_k) \\
&= {}^o\dot{\boldsymbol{r}}_{k-1} + {}^o\boldsymbol{\omega}_k \times {}^o\boldsymbol{R}_{k-1} {}^{k-1}\boldsymbol{c}_k \\
&\qquad \text{since } {}^o\boldsymbol{\omega}_k = {}^o\boldsymbol{\omega}_{k-1} + {}^o\boldsymbol{R}_{k-1} {}^{k-1}\boldsymbol{\omega}_k \\
&= {}^o\dot{\boldsymbol{r}}_{k-1} + {}^o\boldsymbol{\omega}_k \times {}^o\boldsymbol{R}_{k-1}\boldsymbol{R}_z(q_k)\boldsymbol{\sigma}_k
\end{aligned}$$

in which

$$
\begin{aligned}
{}^{o}\boldsymbol{\omega}_k &= {}^{o}\boldsymbol{\omega}_{k-1} + \dot{q}_k({}^{o}\boldsymbol{z}_{k-1}) \\
{}^{o}\dot{\boldsymbol{r}}_{k-1} &= {}^{o}\dot{\boldsymbol{r}}_{k-2} + {}^{o}\boldsymbol{\omega}_{k-1} \times ({}^{o}\boldsymbol{r}_{k-1} - {}^{o}\boldsymbol{r}_{k-2})
\end{aligned}
$$

where ${}^{o}\boldsymbol{z}_{k-1}$ means the z-direction (or driving axis) vector of the $(k-1)$th link frame represented on body center frame. For instance, for $k = 1$ (first link of ith limb)

$$
\begin{aligned}
{}^{o}\dot{\boldsymbol{c}}_{i,1} &= {}^{o}\dot{\boldsymbol{r}}_0 + {}^{o}\boldsymbol{\omega}_1 \times {}^{o}\boldsymbol{R}_0 \boldsymbol{R}_z(q_1)\boldsymbol{\sigma}_1 \\
&= \dot{q}_1[{}^{o}\boldsymbol{z}_0 \times {}^{o}\boldsymbol{R}_0 \boldsymbol{R}_z(q_1)\boldsymbol{\sigma}_1]
\end{aligned}
$$

for $k = 2$ (second link of the ith limb)

$$
\begin{aligned}
{}^{o}\dot{\boldsymbol{c}}_{i,2} &= {}^{o}\dot{\boldsymbol{r}}_1 + {}^{o}\boldsymbol{\omega}_2 \times {}^{o}\boldsymbol{R}_1 \boldsymbol{R}_z(q_2)\boldsymbol{\sigma}_2 \\
&= \dot{q}_1[{}^{o}\boldsymbol{z}_0 \times ({}^{o}\boldsymbol{r}_1 - {}^{o}\boldsymbol{r}_0 + {}^{o}\boldsymbol{R}_1 \boldsymbol{R}_z(q_2)\boldsymbol{\sigma}_2)] \\
&\quad + \dot{q}_2[{}^{o}\boldsymbol{z}_1 \times {}^{o}\boldsymbol{R}_1 \boldsymbol{R}_z(q_2)\boldsymbol{\sigma}_2]
\end{aligned}
$$

for $k = n_i$ (last link of the ith limb)

$$
\begin{aligned}
{}^{o}\dot{\boldsymbol{c}}_{i,n_i} &= {}^{o}\dot{\boldsymbol{r}}_{n_i-1} + {}^{o}\boldsymbol{\omega}_{n_i} \times {}^{o}\boldsymbol{R}_{n_i-1} \boldsymbol{R}_z(q_{n_i})\boldsymbol{\sigma}_{n_i} \\
&= \dot{q}_1[{}^{o}\boldsymbol{z}_0 \times ({}^{o}\boldsymbol{r}_{n_i-1} - {}^{o}\boldsymbol{r}_0 + {}^{o}\boldsymbol{R}_{n_i-1} \boldsymbol{R}_z(q_{n_i})\boldsymbol{\sigma}_{n_i})] \\
&\quad + \dot{q}_2[{}^{o}\boldsymbol{z}_1 \times ({}^{o}\boldsymbol{r}_{n_i-1} - {}^{o}\boldsymbol{r}_1 + {}^{o}\boldsymbol{R}_{n_i-1} \boldsymbol{R}_z(q_{n_i})\boldsymbol{\sigma}_{n_i})] \\
&\quad + \cdots \\
&\quad + \dot{q}_{n_i}[{}^{o}\boldsymbol{z}_{n_i-1} \times {}^{o}\boldsymbol{R}_{n_i-1} \boldsymbol{R}_z(q_{n_i})\boldsymbol{\sigma}_{n_i}].
\end{aligned}
$$

Since the CoM position of the ith limb represented on the body center frame is expressed by (27), the derivative of (27) has the following form:

$$
{}^{o}\dot{\boldsymbol{c}}_i = \sum_{k=1}^{n_i} \mu_{i,k}\, {}^{o}\dot{\boldsymbol{c}}_{i,k}.
$$

Hence,

$$
{}^{o}\dot{\boldsymbol{c}}_i = [\boldsymbol{j}_1, \boldsymbol{j}_2, \ldots, \boldsymbol{j}_{n_i}] \begin{bmatrix} \dot{q}_1 \\ \dot{q}_2 \\ \vdots \\ \dot{q}_{n_i} \end{bmatrix} \triangleq {}^{o}\boldsymbol{J}_{c_i} \dot{\boldsymbol{q}}_i
$$

where

$$
\begin{aligned}
\boldsymbol{j}_1 &\triangleq \sum_{k=1}^{n_i} \mu_{i,k} \{ {}^{o}\boldsymbol{z}_0 \times ({}^{o}\boldsymbol{r}_{k-1} - {}^{o}\boldsymbol{r}_0 + {}^{o}\boldsymbol{R}_{k-1} \boldsymbol{R}_z(q_k)\boldsymbol{\sigma}_k) \} \\
\boldsymbol{j}_2 &\triangleq \sum_{k=2}^{n_i} \mu_{i,k} \{ {}^{o}\boldsymbol{z}_1 \times ({}^{o}\boldsymbol{r}_{k-1} - {}^{o}\boldsymbol{r}_1 + {}^{o}\boldsymbol{R}_{k-1} \boldsymbol{R}_z(q_k)\boldsymbol{\sigma}_k) \} \\
&\vdots \\
\boldsymbol{j}_{n_i} &\triangleq \mu_{i,n_i} \{ {}^{o}\boldsymbol{z}_{n_i-1} \times ({}^{o}\boldsymbol{R}_{n_i-1} \boldsymbol{R}_z(q_{n_i})\boldsymbol{\sigma}_{n_i}) \}.
\end{aligned}
$$

Therefore,

$$
\therefore \quad {}^{o}\boldsymbol{J}_{c_i} = [\boldsymbol{j}_1, \boldsymbol{j}_2, \ldots, \boldsymbol{j}_{n_i}].
$$

REFERENCES

[1] Y. Choi, D. Kim, and B. J. You, “On the walking control for humanoid robot based on the kinematic resolution of CoM Jacobian with embedded motion,” in *Proc. IEEE Int. Conf. Rob. Autom.*, 2006, pp. 2655–2660.

[2] K. Hirai, M. Hirose, Y. Haikawa, and T. Takenaka, “The development of Honda humanoid robot,” in *Proc. IEEE Int. Conf. Rob. Autom.*, 1998, pp. 1321–1326.

[3] Q. Huang, K. Yokoi, S. Kajita, K. Kaneko, H. Arai, N. Koyachi, and K. Tanie, “Planning walking patterns for a biped robot,” *IEEE Trans. Rob. Autom.*, vol. 17, no. 3, pp. 280–289, Jun. 2001.

[4] S. Kajita, K. Y. A. M. Saigo, and K. Tanie, “Balancing a humanoid robot using backdrive concerned torque control and direct angular momentum feedback,” in *Proc. IEEE Int. Conf. Rob. Autom.*, 2001, pp. 3376–3382.

[5] S. Kajita, F. Kanehiro, K. Kaneko, K. Fujiwara, K. Harada, K. Yokoi, and H. Hirukawa, “Biped walking pattern generation by using preview control of zero-moment point,” in *Proc. IEEE Int. Conf. Rob. Autom.*, 2003, pp. 1620–1626.

[6] A. Takanishi, H. Lim, M. Tsuda, and I. Kato, “Realization of dynamic biped walking stabilized by trunk motion on a sagittally uneven surface,” in *Proc. IEEE/RSJ Int. Conf. Intell. Rob. Syst.*, 1990, pp. 323–330.

[7] L. Sentis and O. Khatib, “Synthesis of whole-body behaviors through hierarchical control of behavioral primitives,” *Int. J. Human. Rob.*, vol. 2, no. 4, pp. 505–518, Dec. 2005.

[8] A. Goswami and V. Kallem, “Rate of change of angular momentum and balance maintenance of biped robots,” in *Proc. IEEE Int. Conf. Rob. Autom.*, 2004, pp. 3785–3790.

[9] K. Harada, S. Kajita, K. Kaneko, and H. Hirukawa, “ZMP analysis for arm/leg coordination,” in *Proc. IEEE Int. Conf. Rob. Autom.*, 2003, pp. 75–81.

[10] S. Kajita, F. Kanehiro, K. Kaneko, K. Fujiwara, K. Harada, K. Yokoi, and H. Hirukawa, “Resolved momentum control: Humanoid motion planning based on the linear and angular momentum,” in *Proc. IEEE Int. Conf. Rob. Autom.*, 2003, pp. 1644–1650.

[11] T. Sugihara and Y. Nakamura, “Whole-body cooperative balancing of humanoid robot uisng COG jacobian,” in *Proc. IEEE/RSJ Int. Conf. Intell. Rob. Syst.*, 2002, pp. 2575–2580.

[12] Y. Choi and W. K. Chung, *PID Trajectory Tracking Control for Mechanical Systems, Lecture Notes in Control and Information Sciences*. Berlin, Germany: Springer, 2004, vol. 298.